1

INTRODUCTION AND REVIEW

1.1 INTRODUCTION TO ULTRASHORT LASER PULSES

This book is about ultrafast laser pulses: what they are, linear and nonlinear optical effects which they experience, methods by which they are generated and measured, and how they can be used for measurement of ultrafast physical processes. Let us begin with a definition of the relevant time units.

$$\begin{aligned}
&1 \text{ nanosecond (ns)} &&= 10^{-9} \text{ s} &&= 0.000000001\text{s} \\
&1 \text{ picosecond (ps)} &&= 10^{-12} \text{ s} &&= 0.000000000001\text{s} \\
&1 \text{ femtosecond (fs)} &&= 10^{-15} \text{ s} &&= 0.000000000000001\text{s} \\
&1 \text{ attosecond} &&= 10^{-18} \text{ s} &&= 0.000000000000000001\text{s}
\end{aligned}$$

To put these very short time units in perspective, it is useful to consider their spatial equivalent. If we could take a snapshot of a 1-s light pulse, this pulse would stretch over a distance of 186,000 miles (or 300,000 km), equal to the speed of light multiplied by 1s. This is roughly three-fourths of the distance from the Earth to the moon, a distance we will consider very slow! Now skipping over milliseconds and microseconds, we arrive at nanoseconds. One nanosecond has a spatial extent of 30 cm (ca. 1 ft). Although still rather slow by the standards of ultrafast optics, the nanosecond is the approximate time scale for high-speed electronic chips and computers. The word *ultrafast* is usually applied to the picosecond time scale and below. A picosecond has an extent of 0.3 mm, roughly the thickness of a business card. Given that typical garden-variety laser beams have beam diameters on the order of a few millimeters, we should perhaps envision pulses a picosecond and shorter not as pencils of light but as pancakes of light! In the visible and near-infrared spectral regions, pulses as

Ultrafast Optics, By Andrew M. Weiner

short as a few femtoseconds can now be generated. The spatial extent of even a 10-fs laser pulse is only 3 μm, much less than the diameter of a human hair.

Pulse durations of a few femtoseconds in the visible are approaching the fundamental pulse-width limitation of roughly one optical cycle (roughly one wavelength in spatial extent). Research into attosecond pulse generation is also under way [1]. One key theme in attosecond pulse generation is the use of highly nonlinear optical frequency-conversion methods to produce radiation at much higher frequencies (much shorter wavelengths), corresponding to extreme ultraviolet (XUV) and x-ray spectral regions. At such frequencies the duration of a single optical cycle (and hence the attainable pulse-width limit) is reduced, making attosecond pulses possible.

In this book we specifically focus on ultrafast optics in visible and lower-frequency spectral bands and on time scales down to femtoseconds. Within this time scale the motions of bound electrons that mediate important laser–matter interactions may usually be viewed as instantaneous. Conversely, attosecond time scales and XUV and x-ray frequencies bring in entirely new physics in which laser–matter interactions are sensitive to the noninstantaneous dynamics of bound electron motions. Attosecond technology and science are in a stage of rapid evolution and will undoubtedly be the subject of future books.

Ultrashort pulses have several related characteristics which make them useful for applications. These include the following:

- *High time resolution*. By definition, the pulse duration is in the picosecond or femtosecond range (or below). This provides very high time resolution for excitation and measurement of ultrafast physical processes in solid-state, chemical, and biological materials.
- *High spatial resolution*. The spatial extent of a short light pulse is given by the pulse duration multiplied by the speed of light. As noted above, for very short pulse durations, the spatial pulse length can be on the order of micrometers. This makes ultrashort pulses useful for some microscopy and imaging applications.
- *High bandwidth*. By the uncertainly principle, the product of the pulse-width times the optical bandwidth must be of order unity (or larger). As the pulse duration decreases, the bandwidth increases correspondingly. Pulses of 100 fs have bandwidths on the order of 10 terahertz (THz), and the shortest visible laser pulses contain so much of the visible spectrum that they appear white. This high-bandwidth feature can be important for optical communications as well as other applications.
- *Potential for high intensity*. For a given pulse energy, the peak power and peak intensity are inversely proportional to the pulse duration. Because the size (hence cost) of high-power lasers usually scales with pulse energy, femtosecond pulse technology can be used to obtain ultrahigh peak intensities at moderate energy levels. Amplified femtosecond pulses have produced peak powers up to the petawatt level (1 petawatt = 10^{15} W) and peak intensities exceeding 10^{20} W/cm^2.

The field of ultrafast optics has traditionally been a highly interdisciplinary one, with a wide range of applications areas. To give a flavor for the nature of application areas, we comment below on a few of the research applications.

Ultrafast Spectroscopy Time-resolved spectroscopy is a very successful and probably the most widespread application of picosecond and femtosecond laser technology. The idea

is that ultrashort laser pulses can be used to make "stop-action" measurements of ultrafast physical processes, just as high-speed (microsecond) electronic flashes have been used starting several decades ago to make such stop-action photographs of bullets traveling through apples and milk droplets splashing into milk bowls [2]. On the femtosecond time scale, macroscopic objects such as bullets and milk droplets are motionless, and therefore ultrafast spectroscopy is best applied to study microscopic processes. Examples include investigations of femtosecond interactions of photoexcited electrons and holes with each other and with lattice vibrations in semiconductor crystals, ultrafast laser-induced melting, photodisassociation and ultrafast solution dynamics of chemical species, and ultrafast internal rearrangements of the large organic molecule bacteriorhodopsin as photons absorbed in the retina initiate the first biochemical steps in the process of vision. The principles of ultrafast spectroscopy are covered in Chapter 9 with examples.

Laser-Controlled Chemistry In a research area closely related to ultrafast spectroscopy, researchers are using specially engineered femtosecond laser waveforms to try to influence the course of photoinduced chemical reactions. In addition to observing ultrafast chemical motions as in time-resolved spectroscopy, the added idea here is to control the motions that take place. Since the intrinsic time scale for nuclear motions in chemical systems is tens to hundreds of femtoseconds, femtosecond laser pulses are a natural tool in pursuing the challenging goal of laser-controlled chemistry.

Frequency Metrology Ultrashort pulses are usually emitted from lasers in the form of periodic trains, which under certain conditions can exhibit very high timing stability and long-term coherence. The spectrum of such a periodic train is a comb of up to hundreds of thousands of discrete spectral lines, which may be stabilized to permit precision measurements of optical frequencies with sub-hertz uncertainties across the optical spectrum. Such stabilized frequency combs are now widely adopted for high-precision frequency metrology and for investigations of precision optical clocks. Related topics are discussed in Section 7.5.

High-Speed Electrical Testing Testing is a key issue in the development of high-speed electronic devices and circuits. Electronic test instrumentation based on established technology is usually slower than advanced high-speed research devices. However, since even the very fastest electronic devices only reach into the picosecond range, ultrafast laser technology offers speed to spare. Thus femtosecond optical pulses have been applied to generate subpicosecond electrical pulses and to measure operation of the highest-speed electronic devices. Ultrafast electrical pulse generation and measurement are discussed in Chapter 10.

Laser–Plasma Interactions Lasers with intensities of $10^{13}\,\mathrm{W/cm^2}$ and above (easily achieved using amplified femtosecond pulses) directed onto solid targets are sufficient to strip electrons from their nuclei, resulting in a laser-generated plasma. On the 100-fs time scale, the resulting free electrons do not have enough time to separate from the ionized nuclei. This provides the opportunity to study solid-density plasmas at temperatures as high as 1 million degrees.

Short-Wavelength Generation High-intensity ultrashort pulses at visible wavelengths can also be used to generate coherent short-wavelength radiation in the vacuum ultraviolet and

x-ray ranges through highly nonlinear harmonic generation processes or by pumping x-ray lasers. Coherent short-wavelength radiation may be important, for example, for imaging microscopic structures such as DNA.

Optical Communications The low-loss transmission window of optical fibers has a bandwidth comparable to that of a 100-fs pulse, and therefore ultrashort-pulse technology may play an important role in optical communications. Subpicosecond pulses have already been used for laboratory experiments demonstrating fiber optic transmission of data at Tbit/s (10^{12} bit/s) rates. Here ultrafast optics technology is important not only for pulse generation but also for signal processing, for data detection, and for the advanced metrology necessary for characterizing and optimizing ultrashort-pulse transmission [3,4]. Ultrashort pulses may also prove important in wavelength-division-multiplexing (WDM) systems in which the fiber bandwidth is carved up into different wavelength bands or channels. For WDM applications it is the large bandwidth of the ultrashort pulse (not the short duration) which is useful, since a single pulse contains enough bandwidth to produce a number of wavelength channels.

Biomedical Applications Ultrashort pulses are finding substantial applications in biomedical imaging. Attractive features include the ability to perform optical imaging within scattering media (e.g., most tissues) and to obtain high-resolution depth information. An example of such an application is discussed in Section 3.3.3. In confocal microscopy significantly improved spatial resolution has been demonstrated by relying on two-photon excitation. The ability of ultrashort pulses to provide high intensity without high pulse energy is important in the use of this technique with sensitive biological samples. In laser-assisted surgical procedures ultrashort pulses may in some cases reduce collateral tissue damage by reducing heat deposition.

Materials Processing High-power lasers are used for a variety of industrial applications, such as cutting and drilling. With continuous-wave or "long"-pulse (nanoseconds) lasers, the minimum feature size and the quality of the cut are limited by thermal diffusion of heat to areas neighboring the laser focus. With femtosecond lasers, materials processing is possible using lower pulse energies, due to the very high peak powers, which lead to new physical mechanisms. This reduces the heat deposited into the sample during the laser machining process and leads to a much cleaner cutting or drilling operation.

1.2 BRIEF REVIEW OF ELECTROMAGNETICS

Since ultrashort laser pulses are made up of light, and light is a form of electromagnetic radiation, we very briefly review Maxwell's equations, which describe all forms of electromagnetic radiation, including light. We use MKS (SI) units here and throughout the book. It is assumed that the reader is already familiar with vector calculus. For a more detailed treatment of electromagnetics, the reader is directed to textbooks on this subject [5,6].

1.2.1 Maxwell's Equations

Maxwell's equations are a set of relationships between the electric field **E** and magnetic field **H** (boldface symbols denote vectors). Inside a medium we must also consider the

Table 1.1 Names and Units of Symbols in Maxwell's Equations

Symbol	Name	Units or Numerical Value
E	Electric field	V m^{-1}
D	Electric flux density	C m^{-2}
H	Magnetic field	A m^{-1}
B	Magnetic flux density	T (or V·s m^{-2})
P	Polarization density	C m^{-2}
M	Magnetization density	A m^{-1}
J	Current density	A m^{-2}
ρ	Charge density	C m^{-3}
ε_0	Permittivity of free space	8.85×10^{-12} F m^{-1} (or C V^{-1} m^{-1})
μ_0	Permeability of free space	$4\pi \times 10^{-7}$ H m^{-1} (or V s^2 m^{-1} C^{-1})

charge density ρ, current density **J**, polarization density **P**, and magnetization density **M**, and in order to include the effect of the fields on the matter, the electric and magnetic flux densities, **D** and **B**, are also introduced. Units for these quantities are given in Table 1.1. Maxwell's equations are then written as follows:

$$\nabla \cdot \mathbf{D} = \rho \tag{1.1}$$

$$\nabla \cdot \mathbf{B} = 0 \tag{1.2}$$

$$\nabla \times \mathbf{E} = \frac{-\partial \mathbf{B}}{\partial t} \tag{1.3}$$

$$\nabla \times \mathbf{H} = \mathbf{J} + \frac{\partial \mathbf{D}}{\partial t} \tag{1.4}$$

The relations defining **D** and **B** are

$$\mathbf{D} = \varepsilon_0 \mathbf{E} + \mathbf{P} \tag{1.5}$$

$$\mathbf{B} = \mu_0 (\mathbf{H} + \mathbf{M}) \tag{1.6}$$

The constants ε_0 and μ_0 are known as the *permittivity* and *permeability* of free space, with the numerical values and units given in Table 1.1. Note also that the symbol ρ refers to the free charge density (i.e., any bound charge density associated with the polarization is not included). Similarly, the current density **J** does not include any currents associated with the motion of bound charges (changes in polarization). In free space we would have $\rho = \mathbf{J} = \mathbf{P} = \mathbf{M} = 0$.

For now we specialize to the case of a linear, isotropic, and source-free medium. By *source-free* we mean that the charge and current densities are zero ($\rho = 0$ and $\mathbf{J} = 0$). By *linear* we mean that the medium response (i.e., the polarization and magnetization) is linear in the applied fields. For the case of the electric field, we write

$$\mathbf{P} = \varepsilon_0 \chi_e \mathbf{E} \tag{1.7}$$

where χ_e is known as the electric susceptibility (dimensionless). Inserting into eq. (1.5), one obtains

$$\mathbf{D} = \varepsilon_0(1 + \chi_e)\mathbf{E} = \varepsilon\mathbf{E} \tag{1.8}$$

The proportionality constant ε is termed the dielectric constant, with

$$\varepsilon = (1 + \chi_e)\,\varepsilon_0 \tag{1.9}$$

Other common terms include the relative dielectric constant ($\varepsilon/\varepsilon_0$) and the index of refraction n, which is commonly used in optics, where

$$n^2 = \frac{\varepsilon}{\varepsilon_0} \tag{1.10}$$

For the case of the magnetic field, we write

$$M = \chi_m H \tag{1.11}$$

where χ_m is the magnetic polarizability. Using eq. (1.6), we obtain

$$\mathbf{B} = \mu_0\,(1 + \chi_m)\mathbf{H} = \mu\mathbf{H} \tag{1.12}$$

In most cases in ultrafast optics, one is interested in nonmagnetic materials, for which $\mathbf{M} = 0$. In this case of zero magnetization, one has

$$\mathbf{B} = \mu_0\mathbf{H} \tag{1.13}$$

Equations (1.7) and (1.11) are examples of constitutive laws, which specify the response of the material to the fields. The form of these equations as written arises because we have assumed both linear and isotropic media (for nonisotropic media, one would need to replace the assumed scalar susceptibilities with tensors). We note that there are many situations in ultrafast optics where these assumptions are not valid. For example, nonlinear optical effects, which we discuss in later chapters, require by definition that $\mathbf{P}$ be a nonlinear function of $\mathbf{E}$.

1.2.2 The Wave Equation and Plane Waves

We now consider electromagnetic wave propagation in linear, isotropic, source-free media. To derive the wave equation, we take the curl of eq. (1.3) and insert eq. (1.4), which, using the stated assumptions and a well-known vector identity,[1] gives the following:

$$\nabla \times \nabla \times \mathbf{E} = \nabla\,(\nabla \cdot \mathbf{E}) - \nabla^2\mathbf{E} = -\mu\varepsilon\frac{\partial^2\mathbf{E}}{\partial t^2} \tag{1.14}$$

[1] The identity is $\nabla \times \nabla \times \mathbf{A} = \nabla(\nabla \cdot \mathbf{A}) - \nabla^2\mathbf{A}$. Note that in Cartesian coordinates ∇^2 has a very simple form, namely $\nabla^2\mathbf{A} = (\partial^2/\partial x^2 + \partial^2/\partial y^2 + \partial^2/\partial z^2)\mathbf{A}$.

Since $\nabla \cdot \mathbf{E} = 0$ also under our conditions, we obtain the wave equation

$$\nabla^2 \mathbf{E} = \mu\varepsilon \frac{\partial^2 \mathbf{E}}{\partial t^2} \tag{1.15}$$

One situation of special interest is the case where the field varies in only one direction, which without loss of generality we take as the z direction. Then the wave equation becomes

$$\frac{\partial^2 \mathbf{E}}{\partial z^2} = \mu\varepsilon \frac{\partial^2 \mathbf{E}}{\partial t^2} \tag{1.16}$$

The general solution takes the form

$$\mathbf{E}(z, t) = \mathbf{E}_0 \left(t - \frac{z}{v} \right) \tag{1.17}$$

where $\mathbf{E}_0$ is a vector in the x–y plane [eq. (1.1) precludes E from having a z-component] and $v = 1/\sqrt{\mu\varepsilon}$. The solution can be verified by plugging back into the wave equation. Equation (1.17) is called a *plane-wave solution*, since the field does not vary in the transverse (x–y) plane. It also represents a traveling wave, since the field propagates in the z direction without changing its form. In the case of a pulsed field, $\mathbf{E}_0(t)$ represents the pulse shape. The propagation velocity is given by v. Note that

$$\frac{1}{\sqrt{\mu_0 \varepsilon_0}} = c \cong 2.998 \times 10^8 \,\mathrm{m\,s^{-1}} \tag{1.18}$$

is the velocity of light in free space. Therefore, for the case most common in optics where $\mu = \mu_0$, the velocity of propagation within a medium is given by

$$v = \frac{c}{n} \tag{1.19}$$

where n is the refractive index according to eq. (1.10). Note also that in deriving eqs. (1.14) to (1.17), we have assumed implicitly that the refractive index n is independent of frequency. When n does have a frequency dependence, this can change the propagation velocity or cause the pulse to distort during propagation. These effects are discussed in Chapter 4.

The case of a sinusoidal solution to the wave equation will be of special importance. Then eq. (1.17) takes the form

$$\mathbf{E}(z, t) = \mathbf{E}_0 \cos(\omega t - kz + \phi) \tag{1.20}$$

where $\mathbf{E}_0$ is now a constant vector, ω is the angular frequency, and the propagation constant k must satisfy the dispersion relation

$$k = \omega\sqrt{\mu\varepsilon} \tag{1.21}$$

or again, assuming that $\mu = \mu_0$,

$$k = \frac{\omega n}{c} \tag{1.22}$$

The wave has a temporal oscillation period equal to $2\pi/\omega$ and a spatial period or wavelength *in the medium* given by $\lambda = 2\pi/k$. The wavelength in free space is denoted λ_0 and is given by

$$\lambda_0 = \frac{2\pi c}{\omega} \tag{1.23}$$

Equation (1.20) represents the ideal case of single frequency or monochromatic laser radiation. It can also be written in the equivalent form

$$\mathbf{E}(z, t) = \mathrm{Re}\left\{\tilde{\mathbf{E}}_\mathbf{0} e^{j(\omega t - kz)}\right\} \tag{1.24}$$

where $\mathrm{Re}\{\cdots\}$ denotes the real part and the phase ϕ has been incorporated into the complex vector $\tilde{\mathbf{E}}_\mathbf{0}$. We refer to this form as complex notation. As we will see shortly, ultrashort light pulses are conveniently described as superpositions of sinusoidal solutions of the form (1.20) or (1.24) with different frequencies.

Finally, we note that similar solutions can be written for propagation in directions other than along z, as follows:

$$\mathbf{E}(\mathbf{r}, t) = \mathrm{Re}\left\{\tilde{\mathbf{E}}_\mathbf{0} e^{j(\omega t - \mathbf{k}\cdot\mathbf{r})}\right\} \tag{1.25}$$

Here $\mathbf{k}$ is the propagation vector; it points along the direction of propagation and its magnitude $k = |\mathbf{k}|$ still satisfies the dispersion relation (1.21).

1.2.3 Poynting's Vector and Power Flow

We also review the expressions for energy flow with electromagnetic waves. To arrive at the required formulas, we form the dot product of eq. (1.3) with $\mathbf{H}$ and subtract from this the dot product of eq. (1.4) with $\mathbf{E}$. Using another vector identity,[2] we find that

$$\nabla \cdot (\mathbf{E} \times \mathbf{H}) + \mathbf{H} \cdot \frac{\partial \mathbf{B}}{\partial t} + \mathbf{E} \cdot \frac{\partial \mathbf{D}}{\partial t} + \mathbf{E} \cdot \mathbf{J} = 0 \tag{1.26}$$

We also make use of the divergence theorem,

$$\int \nabla \cdot \mathbf{A}\, dV = \int \mathbf{A} \cdot \hat{\mathbf{n}}\, dS \tag{1.27}$$

which states that the surface integral of a vector $\mathbf{A}$ over a closed surface is equal to the volume integral of $\nabla \cdot \mathbf{A}$ over the volume bounded by that surface. $\hat{\mathbf{n}}$ is the unit vector

[2] The identity is $\nabla \cdot \mathbf{A} \times \mathbf{B} = \mathbf{B} \cdot \nabla \times \mathbf{A} - \mathbf{A} \cdot \nabla \times \mathbf{B}$.

normal to the surface and pointing outward. The result is

$$\int (\mathbf{E} \times \mathbf{H}) \cdot \hat{\mathbf{n}}\, dS + \int dV \left\{ \mathbf{H} \cdot \frac{\partial \mathbf{B}}{\partial t} + \mathbf{E} \cdot \frac{\partial \mathbf{D}}{\partial t} + \mathbf{E} \cdot \mathbf{J} \right\} = 0 \tag{1.28}$$

Finally, assuming a linear medium and substituting for $\mathbf{D}$ and $\mathbf{B}$ using eqs. (1.8) and (1.12), we obtain

$$\int (\mathbf{E} \times \mathbf{H}) \cdot \hat{\mathbf{n}}\, dS + \int dV \left\{ \frac{\partial \left(\frac{1}{2} \varepsilon |\mathbf{E}|^2 \right)}{\partial t} + \frac{\partial \left(\frac{1}{2} \mu |\mathbf{H}|^2 \right)}{\partial t} + \mathbf{E} \cdot \mathbf{J} \right\} = 0 \tag{1.29}$$

Equations (1.28) and (1.29) are representations of Poynting's theorem, which describes conservation of energy in electromagnetic systems. We can identify specific meanings for each of the terms. Look at eq. (1.29), for example:

- $\int (\mathbf{E} \times \mathbf{H}) \cdot \hat{\mathbf{n}}\, dS$ is the net rate of energy flow out of the closed surface. It has units of power (watts). $\mathbf{E} \times \mathbf{H}$ is called the *Poynting vector* and has units of intensity (W/m^2). It gives the power density carried by an electromagnetic wave and the direction in which power is carried.
- $\frac{1}{2} \varepsilon |\mathbf{E}|^2$ and $\frac{1}{2} \mu |\mathbf{H}|^2$ are the local energy densities (J/m^3) associated with the electric and magnetic fields, respectively. $\partial / \partial t \int \frac{1}{2} \varepsilon |\mathbf{E}|^2\, dV$ and $\partial / \partial t \int \frac{1}{2} \mu |\mathbf{H}|^2\, dV$ represent the time rate of change of electric and magnetic field energy stored within the volume, respectively.
- $\int \mathbf{E} \cdot \mathbf{J}\, dV$ represents power dissipation or generation within the volume (in watts). When $\mathbf{E} \cdot \mathbf{J}$ is positive, this term represents power dissipation due, for example, to ohmic losses. Energy is transferred out of the fields and into the medium, typically as heat. When $\mathbf{E} \cdot \mathbf{J}$ is negative, this term represents power supplied by the currents and fed into the electromagnetic fields.

Overall, Poynting's theorem is a power balance equation, showing how changes in stored energy are accounted for by power dissipation and energy flow.

It is worth specializing once more to the case of single-frequency sinusoidal fields, with $\mathbf{E}$ given by eq. (1.25). The $\mathbf{H}$ field is obtained using eq. (1.3), with the result

$$\mathbf{H} = \mathrm{Re} \left\{ \sqrt{\frac{\varepsilon}{\mu}} \frac{\mathbf{k} \times \tilde{\mathbf{E}}_0}{k} e^{j(\omega t - \mathbf{k} \cdot \mathbf{r})} \right\} \tag{1.30}$$

Thus $\mathbf{H}$ is perpendicular to both $\mathbf{E}$ and $\mathbf{k}$, and its magnitude is equal to $\sqrt{\varepsilon / \mu}\, |\mathbf{E}|$. The factor $\sqrt{\mu / \varepsilon}$ is termed the *characteristic impedance* of the medium, and $\sqrt{\varepsilon / \mu}$ is therefore the *admittance*.

In optics one is usually interested in the time-average power flow. This is calculated in complex notation as follows. First consider scalar functions $f(t)$ and $g(t)$, where

$$f(t) = \mathrm{Re}\left\{\tilde{f}e^{j\omega t}\right\} \qquad \text{and} \qquad g(t) = \mathrm{Re}\left\{\tilde{g}e^{j\omega t}\right\} \tag{1.31}$$

The time average of $f(t)g(t)$ is given by

$$\langle fg\rangle = \frac{1}{2}\mathrm{Re}\left\{\tilde{f}\tilde{g}^*\right\} \tag{1.32}$$

Here $\langle\cdots\rangle$ denotes the time average and * indicates a complex conjugate. Similarly, if $\mathbf{f(t)}$, $\mathbf{g(t)}$, $\tilde{\mathbf{f}}$, and $\tilde{\mathbf{g}}$ now denote vectors, the time average of $\mathbf{f}\times\mathbf{g}$ is given by

$$\langle \mathbf{f}\times\mathbf{g}\rangle = \frac{1}{2}\mathrm{Re}\left\{\tilde{\mathbf{f}}\times\tilde{\mathbf{g}}^*\right\} \tag{1.33}$$

Using these relations, the time-average Poynting vector for the plane waves of eqs. (1.25) and (1.30) becomes

$$\langle \mathbf{E}\times\mathbf{H}\rangle = \frac{1}{2}\sqrt{\frac{\varepsilon}{\mu}}\left|\tilde{\mathbf{E}}_\mathbf{0}\right|^2\frac{\mathbf{k}}{k} \tag{1.34}$$

where we have assumed that ε and μ are real. Power is carried along the direction of $\mathbf{k}$. In the case of a nonmagnetic material, we can write the magnitude of the time-average Poynting vector, commonly called the *intensity I*, in the following useful form:

$$I = |\langle \mathbf{E}\times\mathbf{H}\rangle| = \frac{1}{2}\varepsilon_0 cn\left|\tilde{\mathbf{E}}_\mathbf{0}\right|^2 \tag{1.35}$$

1.3 REVIEW OF LASER ESSENTIALS

We will shortly discuss in some detail methods by which lasers can be made to produce ultrashort light pulses. First, however, we give a brief and simple review of lasers in general. More detail can be found in texts on lasers, such as [7,8].

1.3.1 Steady-State Laser Operation

Schematic drawings of two simple laser geometries are shown in Fig. 1.1. Both lasers consist of a set of mirrors and a gain medium. The gain medium is an optical amplifier which coherently amplifies light passing through it. The mirrors may be curved or planar and together make up the laser cavity or resonator. The cavity is aligned so that light reflects back and forth again and again, passing along the same path every time. If we imagine even a very weak light intensity in the cavity (due to spontaneous emission from the gain medium), then for sufficiently high gain, the intensity increases from one round trip through the laser to the next, eventually resulting in an intense beam. In steady state the gain per round trip must equal the loss. Part of the light passes through the partially transmissive output coupler, and this forms the output laser beam, which can be used for experiments.

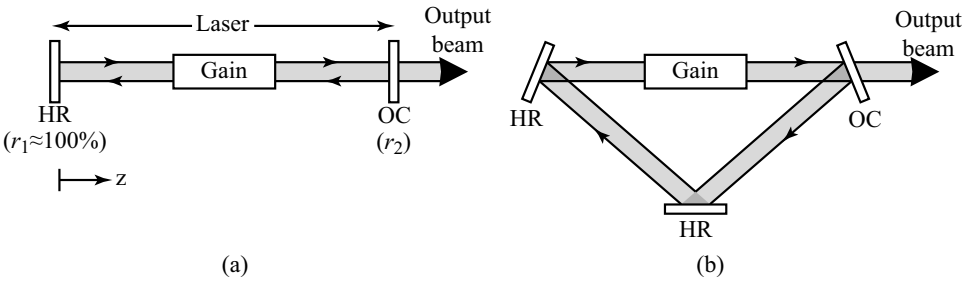

Figure 1.1 Schematic of (a) a linear cavity laser and (b) a ring laser. HR, high reflector; OC, output coupler.

In the linear or Fabry–Perot laser cavity shown in Fig. 1.1a, light passes along the same path, traveling from left to right and right to left. The light makes two passes through the gain medium per round trip. In the ring cavity shown in Fig. 1.1b, light passes through the gain medium only once per round trip. In the diagram we have assumed unidirectional operation (i.e., light is traveling around the ring in only one direction). In real ring lasers either unidirectional or bidirectional operation is possible. Both linear and ring geometries have been used in femtosecond laser design.

For our purposes we usually consider the gain medium as a black box. The physics of laser gain media is usually analyzed using quantum mechanics in courses on laser fundamentals. Here we usually stick to a classical description, although we will use the indispensable energy-level concept, which does come from quantum mechanics. Common laser media used for ultrafast lasers include impurity-doped crystals or glasses such as Ti:sapphire, Nd:YAG or Nd:glass, organic dyes, doped optical fibers, and semiconductor heterojunction diodes. Note that in thermodynamic equilibrium, materials can absorb light but cannot amplify it. To achieve gain, power must be supplied to the medium to promote electrons into excited-state energy levels. When the electrons are "pumped" to the excited state at a sufficiently high rate (i.e., when enough power is supplied), a *population inversion*, in which the population of electrons in an excited energy level exceeds that in a lower level, can be achieved. A population inversion is a necessary condition to achieve optical gain. Power can be supplied to the laser medium in many different ways. Optical pumping, in which absorption of pump photons from a flashlamp or an external laser promotes the electrons to the excited state, is often used in ultrashort-pulse lasers. Other pumping methods include current injection in semiconductor diode lasers or electric discharges in gas lasers. The need for a pump source to obtain optical gain can be likened to the need to plug in an electronic amplifier.

To achieve steady-state laser operation, the electric field must repeat itself after a round trip through the laser cavity. Therefore, let us now consider a single round trip of a monochromatic field through a cavity. To be specific, we consider the linear cavity of Fig. 1.1a. The optical path length between mirrors is denoted l; the total optical path length is therefore $2l$. The electric field amplitude of a monochromatic plane wave propagating the $+z$ direction can be written

$$E(z, t) = \mathrm{Re}\left\{ E_0 e^{j(\omega t - kz)} \right\} \tag{1.36}$$

where the field is now taken as a scalar for convenience. E_0 is the field amplitude just to the right of the high reflector at $z = 0$, ω is the angular frequency, $k = \omega n/c$ is the propagation constant, and $n = n' + jn''$ is the complex refractive index (n' and n'' are both real numbers). The field just before the output coupler is written

$$E = \mathrm{Re}\left\{ E_0 e^{(\omega/c)n''l_g} e^{j\omega t} e^{-j(\omega/c)(n'l_g + l_a)} \right\} \tag{1.37}$$

In eq. (1.37) n' and n'' refer to the gain medium; the regions outside the gain medium are taken as air, with $n = 1$. l_g and l_a are the physical lengths of the gain medium and air region, respectively. We can now identify $l = n'l_g + l_a$ as the optical path length. We also see that for $n'' > 0$, the field has been amplified.

The field at $z = 0$, corresponding to a round-trip path through the resonator, is obtained by reflecting off the output coupler with amplitude r_2, passing back through the cavity, and then reflecting off the high reflector with amplitude r_1. Although ideally we would have $r_1 = 100\%$, we keep the variable r_1 in our expressions to account for any imperfections of the high reflector as well as any other losses in the laser cavity besides those arising from the output coupler. The resulting expression for the field is as follows:

$$E = \mathrm{Re}\left\{ r_1 r_2 e^{2(\omega/c)n''l_g} E_0 e^{j\omega t} e^{-j(2\omega/c)l} \right\} \tag{1.38}$$

To satisfy the steady-state requirement, eq. (1.38) must be equal to the initial field, eq. (1.36), evaluated at $z = 0$: $E = \mathrm{Re}\left[E_0 e^{j\omega t}\right]$. This leads to two conditions: the gain condition and the phase condition. The *gain condition*,

$$r_1 r_2 e^{(2\omega/c)n''l_g} = 1 \tag{1.39}$$

states that the round-trip gain exactly balances the round-trip loss. The *phase condition*,

$$\frac{2\omega l}{c} = 2m\pi \tag{1.40}$$

requires that the the round-trip phase shift is equal to an integer m times 2π. This means that the laser is only allowed to oscillate at certain discrete angular frequencies, given by

$$\omega_m = \frac{m\pi c}{l} \tag{1.41}$$

These frequencies are known as the *longitudinal modes* of the cavity. In terms of the frequency $f = \omega/2\pi$, the mode frequencies are

$$f_m = \frac{mc}{2l} \tag{1.42}$$

and the mode spacing (taking n' as frequency independent) is

$$\Delta f = f_m - f_{m-1} = \frac{c}{2l} \tag{1.43}$$

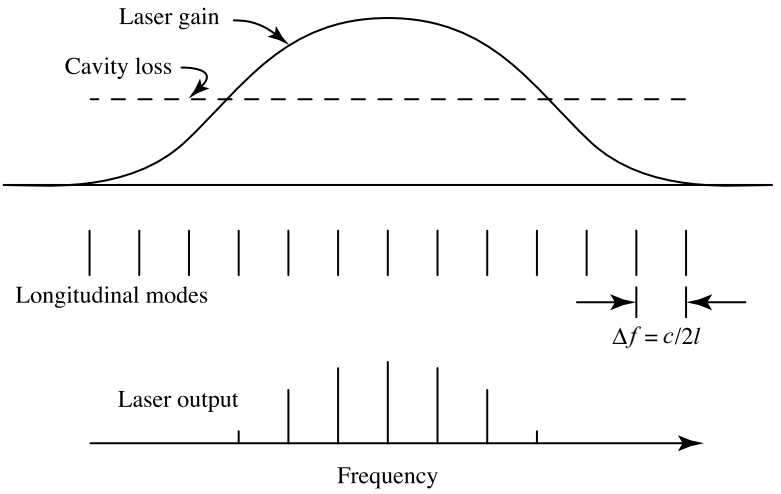

Figure 1.2 Laser gain and cavity loss spectra, longitudinal mode locations, and laser output for multimode laser operation.

A frequency-domain view of basic laser operation is pictured schematically in Fig. 1.2. A comparison of the gain vs. loss is shown at the top, with the locations of the longitudinal modes shown below. The resonator loss is taken as frequency independent, while the gain is assumed to have a bandpass spectral response. Laser oscillation occurs only for those modes where the gain lies above the loss line. In the situation shown, gain exceeds loss for several longitudinal modes, and multiple output frequencies appear simultaneously. This is called *multimode operation*.

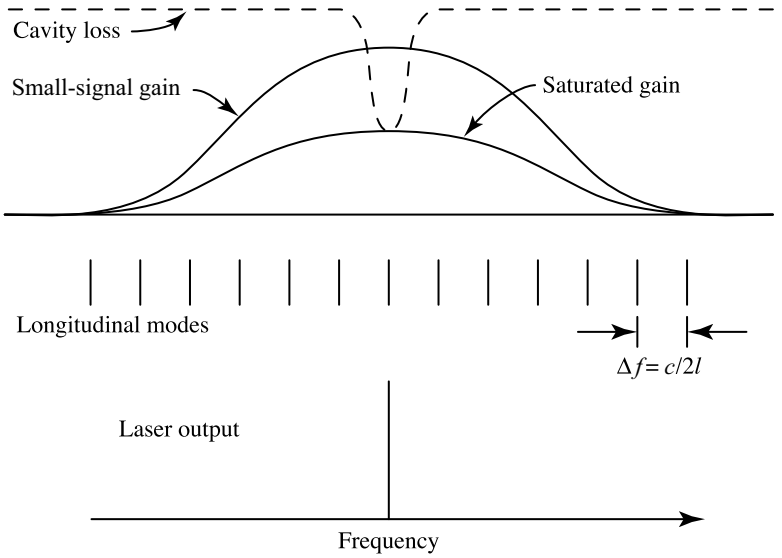

Figure 1.3 Gain and loss spectra, longitudinal mode locations, and output of a homogeneously broadened laser under single-mode operation.

To obtain monochromatic or single-mode laser radiation, it is usually necessary to insert a frequency-dependent loss element (a filter) to ensure that gain exceeds loss for only a single longitudinal mode. This situation is sketched in Fig. 1.3. Note, however, that the steady-state laser gain condition [eq. (1.39)] requires that the gain exactly equal rather than exceed the loss. For this reason we now distinguish between small-signal gain and saturated gain. *Small-signal gain* is gain available under conditions of zero or at least very weak light intensity and depends only on the properties of the laser medium and the pump level. For weak spontaneous emission to build up to produce a significant laser intensity, the small-signal gain must indeed exceed the loss. However, as the intracavity intensity increases, the small-signal condition is violated. As laser photons are amplified in the laser medium through stimulated emission, at the same time electrons in the excited energy state are stimulated back down to the lower-energy state. The intracavity field extracts energy that was stored in the gain medium by the pump and reduces the number of excited-state electrons available for amplification. As a result, the gain is reduced. The actual gain that results, known as the *saturated gain*, depends on the properties of the laser medium, the pump level, and the intracavity laser intensity. Note that saturation phenomena are quite familiar in the context of electronic amplifiers, where the full amplifier gain is available only for input signals below a certain voltage level; for higher voltage levels the output may appear to be clipped.

To clarify the role of gain saturation in lasers, let us imagine that the pump intensity is increased slowly from zero in a single-mode laser cavity. As long as the small-signal gain remains below the loss, the laser intensity is zero. When the pump intensity is sufficient to raise the small-signal gain to equal the loss exactly, the laser reaches *threshold*. The laser power is still zero at this point. When the pump is increased above threshold, the laser power increases, and this saturates the gain. For a given pump level, the laser intensity builds up just enough to maintain the saturated gain at exactly the loss level, as pictured in Fig. 1.3. Thus, pump power above the threshold value is converted into stimulated emission. As a result, the laser intensity increases linearly with pump power above threshold.

In our discussion we have implicitly assumed that the gain medium is broadened homogeneously. This means that all the excited-state electrons have identical gain spectra, so that the overall gain is simply the gain spectrum per electron times the population difference between upper and lower laser states. Gain saturation in a homogeneously broadened medium results from a decrease in this population difference, and therefore the saturated gain has the same spectral shape as the small-signal gain.

Inhomogeneously broadened media and inhomogeneously broadened lasers, in which different excited-state electrons have different spectra, are also possible. This may result, for example, due to the fact that different impurity ions in a glass laser experience different local environments. As shown in Fig. 1.4a, the overall absorption or gain spectrum is then determined by both the individual homogeneous lines (associated with electrons with identical resonance frequencies) and the inhomogeneous distribution function $G(\omega - \Omega_0)$. When the inhomogeneous distribution is wide compared to the homogeneous linewidth, the net absorption or gain spectrum is determined mainly by $G(\omega - \Omega_0)$ and peaks at the center of the inhomogeneous distribution Ω_0. As shown in Fig. 1.4b, the saturation behavior of an inhomogeneously broadened medium interacting with a narrow-bandwidth laser field is quite different than saturation behavior for homogeneous broadening. In particular, saturation induces a "spectral hole" in the vicinity of the laser field, while the spectrum is essentially unchanged for frequencies much more than a homogeneous linewidth away from the laser frequency. Because inhomogeneously broadened lasers are not in common use for ultrashort

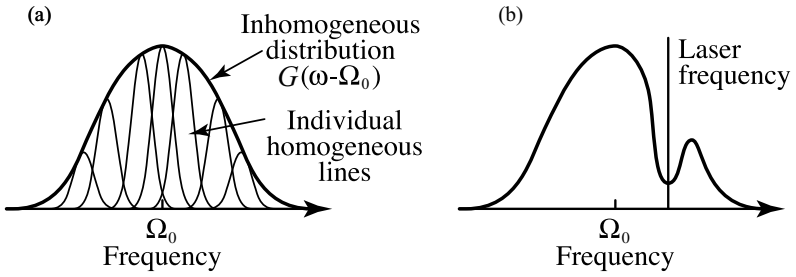

Figure 1.4 (a) Absorption or gain spectrum of a medium with an inhomogeneous distribution $G(\omega - \Omega_0)$ of transition frequencies; (b) spectral hole burning associated with saturation of an inhomogeneously broadened medium by a narrowband laser field.

pulse generation, we do not discuss them further at this time. However, we return to this topic in Chapter 9, where we discuss line-shape theory and ultrafast spectroscopy techniques for probing physics associated with homogeneous and inhomogeneous broadening.

1.3.2 Gain and Gain Saturation in Four-Level Atoms

To provide further insight, we discuss gain saturation for the four-level atom. The four-level atom approximation, sketched in Fig. 1.5, is commonly used to model important mode-locking media such as Ti:sapphire or dye molecules. Here we discuss continuous-wave (CW) saturation; saturation in response to pulses is covered in Chapter 2. Note that we do not mean the word *atom* in the term *four-level atom* literally. Rather, this word refers to whatever entity (molecule, impurity complex, etc.) is active in the laser gain process.

Referring to Fig. 1.5, electrons are promoted from the lowest state, denoted level 1, up to level 2 (e.g., via optical pumping). Electrons in level 2 are usually assumed to relax very rapidly to level 3, so that the population of electrons in level 2 remains close to zero. Physically, this relaxation usually arises from vibronic rearrangement of the nuclei within the crystal-impurity or molecular system, which typically occurs on a subpicosecond time scale following the electronic transition from 1 to 2. The transition from 3 to 4 is the lasing transition, and levels 3 and 4 are the upper and lower laser levels, respectively. Electrons from level 3 can undergo stimulated emission down to level 4, giving up a photon to the laser field in the process, or they can also relax spontaneously down to level 4 with rate τ_G^{-1}, in which case their energy is not available to the laser field. τ_G is the energy storage time of the gain medium, which may range from nanoseconds to milliseconds in materials used for femtosecond pulse generation. Electrons in level 4 are again assumed to relax very rapidly

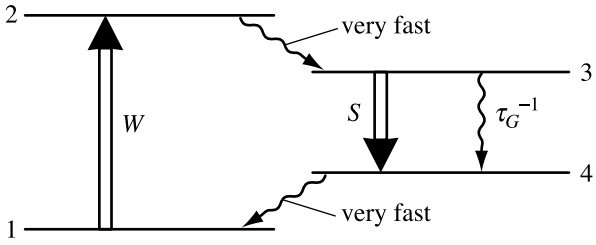

Figure 1.5 Energy-level structure for a four-level atom.

back to level 1, so that the lower laser level remains nearly empty (this is the principal advantage of four-level atoms).

Mathematically, we denote the total density of atoms (in m^{-3}) as N_G, and the number density in each of the four levels as N_1, N_2, N_3, and N_4, respectively. Naturally, we have

$$N_1 + N_2 + N_3 + N_4 = N_G \tag{1.44}$$

The level populations are described by the following rate equations:

$$\dot{N}_1 = -W(N_1 - N_2) + \frac{N_4}{\tau_{41}} \tag{1.45}$$

$$\dot{N}_2 = W(N_1 - N_2) - \frac{N_2}{\tau_{23}} \tag{1.46}$$

$$\dot{N}_3 = -S(N_3 - N_4) - \frac{N_3}{\tau_G} + \frac{N_2}{\tau_{23}} \tag{1.47}$$

$$\dot{N}_4 = S(N_3 - N_4) - \frac{N_4}{\tau_{41}} + \frac{N_3}{\tau_G} \tag{1.48}$$

Here W is the pumping rate per atom (in s^{-1}) from level 1 to 2, and its strength is controlled via the external excitation of the laser medium. For example, in the case of optical pumping, W is proportional to the intensity of the pump laser. S is the stimulated emission rate per atom (in s^{-1}), which is proportional to intensity and given in physical units by

$$S = \frac{\sigma_{34} I(\omega_{34})}{\hbar\omega_{34}} \tag{1.49}$$

Here σ_{34} is the "cross section" of the laser transition, which characterizes the strength of the laser–matter interaction, $I(\omega_{34})$ is the laser intensity inside the resonator, and $\hbar\omega_{34}$ gives the photon energy of the $3 \rightarrow 4$ transition. In the case of optical pumping, a similar expression applies for W. τ_{23} and τ_{41} are the $2 \rightarrow 3$ and $4 \rightarrow 1$ relaxation times, respectively. The gain is proportional to the population difference between the laser levels:

$$g = \frac{\sigma_{34}}{2}(N_3 - N_4) l_g \tag{1.50}$$

The factor of $1/2$ arises because we have written the gain coefficient for the *field* in eq. (1.50); this factor is not present when writing the gain coefficient for the *intensity*. In steady state all the time derivatives in the rate equations are set to zero. Furthermore, since the relaxation from levels 2 and 4 is very fast, we can also approximate $N_1 - N_2 = N_1$ and $N_3 - N_4 = N_3$ in eqs. (1.45 to 1.48). Solving for the upper-laser-level population under these conditions yields the following expression for the gain:

$$g = \left(\frac{1}{2}\right) \frac{\sigma_{34} W N_G \tau_G l_g}{1 + (W + S)\tau_G} \tag{1.51}$$

The gain is a function of both W and S. In the small-signal regime ($S = 0$), the small-signal gain g_0 is given by

$$g_0 = \left(\frac{1}{2}\right) \frac{\sigma_{34} W N_G \tau_G l_g}{1 + W\tau_G} \tag{1.52}$$

g_0 starts at zero, then increases linearly with pump rate W at first but saturates for large W when N_3 approaches N_G. In the large-signal regime (S is finite), the gain can be rewritten

$$g = \frac{g_0}{1 + S/S_{\text{sat}}} \tag{1.53}$$

where

$$S_{\text{sat}} = W + \frac{1}{\tau_G} \tag{1.54}$$

is a saturation parameter. Within a laser, the gain first increases with increasing pump until threshold is reached. Above threshold the small-signal gain g_0 continues to increase as W increases, but the actual gain g is clamped or saturated at the value needed for threshold, which we denote g_{th}. The laser intensity (inside the laser) is found by setting eq. (1.53) to g_{th}, with the result

$$S = S_{\text{sat}} \left(\frac{g_0}{g_{\text{th}}} - 1\right) \tag{1.55}$$

Lasing can occur in three-level systems as well as in the four-level systems discussed above. For further discussion, see standard laser texts.

1.3.3 Gaussian Beams and Transverse Laser Modes

Real laser beams have a finite transverse extent; they are not plane waves. In most cases of interest to us, however, laser beams may be considered paraxial. This means that they are made up of a superposition of plane waves with propagation vectors close to a single direction (which we take as z). Equivalently, the variation of the field in the transverse (x–y) direction must be much weaker than in the z direction. Under these conditions the electric field vector still lies mainly in the x–y plane. In the following we give a brief summary of paraxial laser beams and the related transverse mode structure of lasers. More detail can be found in most texts on lasers (e.g., [7–9]).

For a monochromatic, paraxial wave it is useful to write

$$E(z, t) = \text{Re}\left\{\tilde{E}_0 u(x, y, z) e^{j(\omega t - kz)}\right\} \tag{1.56}$$

where k is given by eq. (1.22) and E refers to a single transverse polarization component. In this form the most rapid wavelength-scale variation of the field is carried by the e^{-jkz}

term; $u(x, y, z)$ is a slowly varying envelope. Substitution into the wave equation, eq. (1.15), yields

$$\nabla_T^2 u + \frac{\partial^2 u}{\partial z^2} - 2jk\frac{\partial u}{\partial z} = 0 \tag{1.57}$$

where $\nabla_T^2 = \partial^2/\partial x^2 + \partial^2/\partial y^2$. Since u is assumed to be slowly varying, $\left|\partial^2 u/\partial z^2\right| \ll 2k\,|\partial u/\partial z|$, and therefore $\partial^2 u/\partial z^2$ can be neglected. The resulting paraxial wave equation is

$$\nabla_T^2 u - 2jk\frac{\partial u}{\partial z} = 0 \tag{1.58}$$

The paraxial wave equation has Gaussian beam solutions that provide a good description of laser beams both inside and outside the laser cavity. A particularly useful solution is written as follows:

$$u_{00}(x, y, z) = \frac{w_0}{w(z)} e^{-(x^2+y^2)/w^2(z)} e^{-jk(x^2+y^2)/2R(z)} e^{j\phi(z)} \tag{1.59}$$

where we define

$$w^2(z) = w_0^2\left[1 + \left(\frac{z}{z_0}\right)^2\right] \tag{1.60a}$$

$$\frac{1}{R(z)} = \frac{z}{z^2 + z_0^2} \tag{1.60b}$$

$$\phi(z) = \tan^{-1}\left(\frac{z}{z_0}\right) \tag{1.60c}$$

$$z_0 = \frac{\pi w_0^2 n}{\lambda} \tag{1.60d}$$

This solution, sketched in Fig. 1.6, describes a beam that comes to a focus at $z = 0$ with a radius w_0 (measured at $1/e$ of the on-axis field). The beam radius $w(z)$ changes only slowly within the region $|z| < z_0$; far outside this region the beam spreads with a half angle equal to $\lambda/\pi w_0 n$. The depth b over which the beam radius remains less than $\sqrt{2}\,w_0$ is given by $b = 2z_0$, where b is termed the depth of focus or the confocal parameter. $R(z)$ is the radius of curvature of the phase fronts. $R = \infty$ at the beam waist ($z = 0$), corresponding to a planar phase front; for $|z| \gg z_0$, the phase fronts become spherical with a center of curvature at $z = 0$. Equation (1.60c) indicates a phase shift that accompanies propagation through the focal region. This Gaussian beam solution describes both laser beam propagation in free space as well as the spatial behavior of the fundamental transverse modes that are allowed inside a laser resonator with flat or spherical mirrors. The particular transverse mode of this

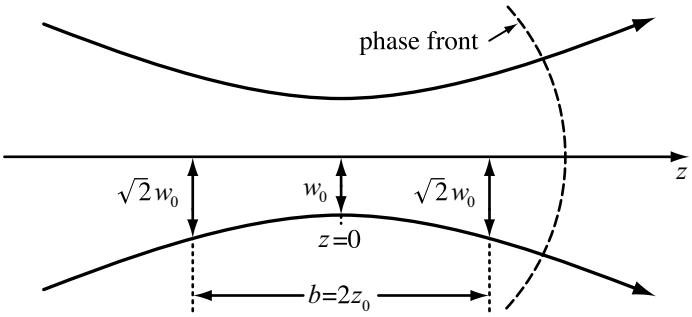

Figure 1.6 Gaussian beam solution of the paraxial wave equation, showing evolution of the beam radius and representative phase front.

type allowed within a given laser resonator is selected by the requirement that $R(z)$ must match the radii of curvature of the mirrors within the laser, which determines the location of the beam waist and the value of w_0; for free propagation outside a laser, any solution of this type is allowed.

It is useful to know the power P carried by a Gaussian beam, which is obtained by integrating the intensity over its cross-sectional area. The result is

$$P = \int dA \, \frac{\varepsilon_0 nc}{2} \left|\tilde{E}_0\right|^2 |u|^2 = \frac{\varepsilon_0 nc}{2} \left|\tilde{E}_0\right|^2 \frac{w_0^2}{w^2(z)} \int_0^\infty 2\pi r \, dr \, e^{-2r^2/w^2(z)}$$
$$= \frac{1}{2}\varepsilon_0 nc \left|\tilde{E}_0\right|^2 \frac{\pi w_0^2}{2} \tag{1.61}$$

The power is equal to the on-axis intensity at the focus, multiplied by the area of a circle of radius $w_0/\sqrt{2}$, which is the radius of the intensity at the e^{-1} point.

Equation (1.59) is the lowest-order member of an entire family of Hermite–Gaussian solutions to the paraxial wave equation, given by

$$u_{mn}(x, y, z) \sim \frac{1}{w(z)} H_m\left(\frac{\sqrt{2}\,x}{w(z)}\right) H_n\left(\frac{\sqrt{2}\,y}{w(z)}\right)$$
$$\times \, e^{-(x^2+y^2)/w^2(z)} e^{-jk(x^2+y^2)/2R(z)} e^{j(m+n+1)\phi(z)} \tag{1.62}$$

The $H_\nu(\xi)$ with ν a nonnegative integer are Hermite polynomials [10], where for example, $H_0(\xi) = 1$, $H_1(\xi) = 2\xi$, and $H_2(\xi) = 4\xi^2 - 2$. In general, the H_ν are polynomials of order ν, which become wider and exhibit a greater number of zero crossings as ν increases. The expressions for $w(z)$, $R(z)$, and $\phi(z)$ are still as given above. Although the fundamental Gaussian beam is by far the most important in most ultrafast optics applications, the higher order ($m \neq 0$ or $n \neq 0$) Hermite–Gaussian solutions will be relevant in our study for several reasons. For example, all the u_{mn} in eq. (1.62) are allowed transverse modes of laser resonators, termed TEM_{mn} *modes*, although the fundamental TEM_{00} mode usually has the lower loss and is therefore favored. We shall see however that higher-order modes were significant in the discovery of the important Kerr lens mode-locking technique for short pulse

generation with solid-state lasers. Additionally, the Hermite–Gaussians form a complete orthogonal basis set, which means that an arbitrary spatial beam profile can be decomposed into a superposition of these functions.

To calculate the propagation of Gaussian beams through linear optical systems, it is convenient to introduce a complex q parameter, such that

$$\frac{1}{q(z)} = \frac{1}{R(z)} - \frac{j\lambda}{\pi w^2(z) n} \tag{1.63}$$

The effect of the optical system can then be characterized by a bilinear transformation of q: namely,

$$q_{\text{out}} = \frac{Aq_{\text{in}} + B}{Cq_{\text{in}} + D} \tag{1.64}$$

The coefficients appearing in eq. (1.64) are usually written in matrix form. The matrices for a few common systems are as follows:

- A length d of a homogeneous medium:

$$\begin{pmatrix} A & B \\ C & D \end{pmatrix} = \begin{pmatrix} 1 & d \\ 0 & 1 \end{pmatrix} \tag{1.65a}$$

- A lens with focal length f (this matrix also applies to a spherical mirror of radius R if we set $f = R/2$):

$$\begin{pmatrix} A & B \\ C & D \end{pmatrix} = \begin{pmatrix} 1 & 0 \\ -1/f & 1 \end{pmatrix} \tag{1.65b}$$

- A planar interface, perpendicular to the propagation direction, from a medium with index n_1 to a medium with index n_2:

$$\begin{pmatrix} A & B \\ C & D \end{pmatrix} = \begin{pmatrix} 1 & 0 \\ 0 & n_1/n_2 \end{pmatrix} \tag{1.65c}$$

An important property of such matrices is that the effect of cascaded systems is computed via matrix multiplication. If $M_1, M_2, \ldots, M_N$ represent the matrices for N cascaded systems, with the beam entering system 1 first and system N last, the effect of the cascaded system is given by $M_N \cdots M_2 M_1$. For example, the matrix for a homogeneous slab of thickness d and index n and surrounded on either side by free space is

$$\begin{pmatrix} A & B \\ C & D \end{pmatrix} = \begin{pmatrix} 1 & 0 \\ 0 & n \end{pmatrix} \begin{pmatrix} 1 & d \\ 0 & 1 \end{pmatrix} \begin{pmatrix} 1 & 0 \\ 0 & 1/n \end{pmatrix} = \begin{pmatrix} 1 & d/n \\ 0 & 1 \end{pmatrix} \tag{1.66}$$

The matrices given above are also useful in the ray optics description of optical systems. Here one writes

$$\begin{pmatrix} x_{\text{out}} \\ x'_{\text{out}} \end{pmatrix} = \begin{pmatrix} A & B \\ C & D \end{pmatrix} \begin{pmatrix} x_{\text{in}} \\ x'_{\text{in}} \end{pmatrix} \tag{1.67}$$

where x_{in} and x'_{in} are the position and slope of the incoming ray, respectively, and similarly for the outgoing ray. For a given optical system, the matrixes for the ray optics description and the Gaussian beam (q parameter) description are identical. The ray optics description is sometimes helpful in identifying or interpreting the *ABCD* matrices. For example, the matrix in eq. (1.66) says that the slab of physical thickness d has an effective thickness of d/n. From the ray optics description, it is clear that this occurs due to bending of the rays toward the normal as they enter the medium.

The q parameter and the *ABCD* matrices are useful in solving for the transverse mode of laser resonators. Assume that we have calculated the matrix for one complete round trip through the resonator, starting, for example, at a particular mirror $\mathcal{M}$. Then one condition for an acceptable transverse mode is that the field pattern must exactly reproduce itself after one round trip, which can be formulated as

$$q = \frac{Aq + B}{Cq + D} \tag{1.68}$$

A further condition is that for a stable mode, the beam radius must be finite, which means that q must have a nonzero imaginary part. From the ray optics perspective, this stability condition means that incoming rays remain confined after many passes through the system. Multiplying through by the denominator in eq. (1.68) yields a quadratic polynomial equation for q. The root of this equation with a negative imaginary part gives q at mirror $\mathcal{M}$, and q in turn yields the mode size within the laser resonator. Not all resonators have stable solutions. A well-known and important example is the simple two-mirror cavity (Fig. 1.7), consisting of mirrors with radii of curvature R_1 and R_2 which are separated by distance d. After calculating the round-trip *ABCD* matrix and requiring that the roots of eq. (1.68) have nonzero imaginary part, one obtains the stability relation

$$0 < \left(1 - \frac{d}{R_1}\right)\left(1 - \frac{d}{R_2}\right) < 1 \tag{1.69a}$$

or simply

$$0 < g_1 g_2 < 1 \tag{1.69b}$$

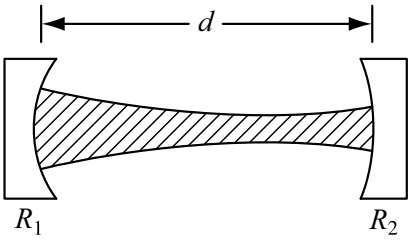

Figure 1.7 Simple two-mirror optical resonator.

where $g_1 = 1 - d/R_1$ and $g_2 = 1 - d/R_2$ are symbols often used to express the stability condition succinctly. We make use of this stability condition when we discuss Kerr lens mode-locking in Chapter 2.

1.4 INTRODUCTION TO ULTRASHORT PULSE GENERATION THROUGH MODE-LOCKING

The single-mode laser discussed in Section 1.3 can have a very narrow optical frequency spectrum. This results in the well-known monochromaticity property of lasers. However, short pulse generation requires a broad optical bandwidth and hence multiple longitudinal mode operation. Even with the bandwidth-limiting filter removed, however, the saturated gain in a homogeneously broadened laser is below the loss level except for those modes near the peak of the gain spectrum, and this also limits the number of oscillating modes. Methods for forcing a great number of modes to oscillate to obtain broad bandwidths and ultrashort pulses are covered in detail later. In the following we analyze the time-domain characteristics of a laser which we assume already has multimode operation.

For a multimode laser we can write the electric field as follows:

$$e(z, t) = \mathrm{Re}\left\{ \sum_m E_m e^{j(\omega_m t - k_m z + \phi_m)} \right\} \tag{1.70a}$$

where

$$\omega_m = \omega_0 + m\,\Delta\omega = \omega_0 + \frac{2m\pi c}{L} \tag{1.70b}$$

and

$$k_m = \frac{\omega_m}{c} \tag{1.70c}$$

Henceforth we use lowercase letters [e.g., $e(z, t)$] for the time-domain representation of the field and capital letters (e.g., E_m) to refer to the frequency domain. Equation (1.70a) most accurately models a unidirectional ring laser, where the z coordinate refers to travel around the ring in the direction of laser oscillation, although the same essential results will also hold for a linear (Fabry–Perot) laser. The round-trip distance around the ring is denoted L (for a Fabry–Perot laser we would use $L = 2l$, where l is the Fabry–Perot mirror separation). In this formulation we are assuming that the laser is oscillating in a single transverse mode, so that the spatial profile may be dropped.

Equation (1.70a) can be rewritten as follows:

$$e(z, t) = \mathrm{Re}\left\{ e^{j\omega_0(t - z/c)} \sum_m E_m e^{j[m\Delta\omega(t - z/c) + \phi_m]} \right\} \tag{1.71a}$$

$$= \mathrm{Re}\left\{ a\left(t - \frac{z}{c}\right) e^{j\omega_0(t - z/c)} \right\} \tag{1.71b}$$

where

$$a\left(t-\frac{z}{c}\right)=\sum_m E_m e^{j[m\Delta\omega(t-z/c)+\phi_m]} \tag{1.71c}$$

Thus, the electric field is the product of a complex envelope function $a\,(t-z/c)$ with the optical carrier $e^{j\omega_0(t-z/c)}$.

This terminology is convenient because in many cases the carrier term, which oscillates with a period of just a few femtoseconds (for visible wavelengths), varies much more rapidly than the envelope function. (However, for the shortest pulses available today, comprising just a few optical cycles, this distinction is blurred.) Both carrier and envelope functions travel around the laser cavity at the speed of light. Furthermore, for a specific location in the cavity (z fixed), the envelope function is periodic with period

$$T=\frac{2\pi}{\Delta\omega}=\frac{2l}{c}=\frac{L}{c} \tag{1.72}$$

This corresponds to the time required for light to make one round trip around the resonator.

If we are to say anything further about the shape of the envelope function, we need to specify the mode amplitudes E_m and phases ϕ_m. If we assume that there are N oscillating modes all with equal amplitudes E_0 and with the phases identically zero, eq. (1.71a) becomes easy to evaluate. The process (discussed later) by which the modes are held with fixed relative phases is known as *mode-locking*, and as we shall see, having all the phases equal is a particularly useful form of mode-locking. Equation (1.71a) now becomes

$$e(z,t)=\mathrm{Re}\left\{E_0 e^{j\omega_0(t-z/c)}\sum_{-(N-1)/2}^{(N-1)/2} e^{j[m\Delta\omega(t-z/c)]}\right\} \tag{1.73}$$

To evaluate this we substitute $m'=m+(N-1)/2$ and use the summation formula

$$\sum_{m=0}^{q-1} a^m=\frac{1-a^q}{1-a} \tag{1.74}$$

Upon some further simplification, the result is

$$e(z,t)=\mathrm{Re}\left\{E_0 e^{j\omega_0(t-z/c)}\frac{\sin\left(N\,\Delta\omega/2\right)(t-z/c)}{\sin\left(\Delta\omega/2\right)(t-z/c)}\right\} \tag{1.75}$$

The laser intensity (I), averaged over an optical cycle, is proportional to $|e(z,t)|^2$. At a specific cavity location, say $z=0$, we have

$$I(t)\sim|E_0|^2\,\frac{\sin^2\left(N\,\Delta\omega t/2\right)}{\sin^2\left(\Delta\omega t/2\right)}. \tag{1.76}$$

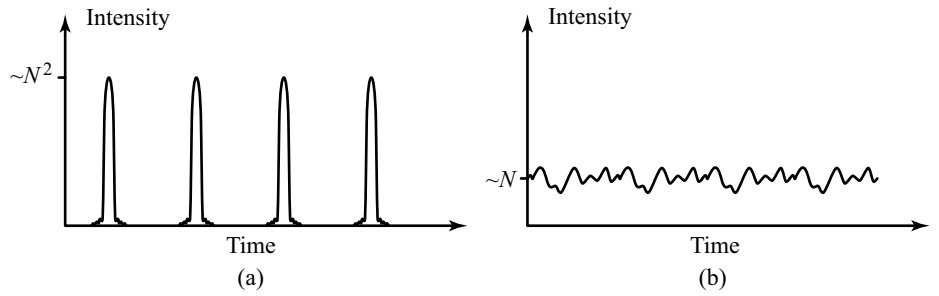

Figure 1.8 (a) Mode-locked laser output with constant mode phase; (b) laser output with randomly phased modes.

The resulting intensity profile is sketched in Fig. 1.8a. Some of the key points are as follows:

- The output consists of a periodic series of short pulses, with period $T = 1/\Delta f = L/c$.
- The pulse duration is approximately $\Delta t = 2\pi/N\,\Delta\omega = 1/N\,\Delta f$. Thus, the pulse duration is equal to the periodicity divided by the number of modes. Equivalently, the pulse width is equal to the inverse of the total laser bandwidth.
- The peak intensity is proportional to $N^2\,|E_0|^2$. In comparison, the average intensity (averaged over the pulse period), given by the number of modes times the power per mode, is proportional to $N\,|E_0|^2$. Thus, the peak intensity of a mode-locked pulse is enhanced by a factor N.

A very different situation arises if we assume that the mode phases are random, as in a garden-variety multimode laser. In this case the intensity profile takes on a random appearance, as shown in Fig. 1.8b. Key points are as follows:

- The intensity fluctuates randomly about the average intensity value. The average intensity is $\sim N\,|E_0|^2$, which is the same as in the mode-locked case, although the peak intensity is a factor of N lower.
- The time scale over which the fluctuations vary (also known as the *correlation time*) is still $\Delta t \approx 1/N\,\Delta f$.
- The intensity fluctuations are still periodic with period $T = 1/\Delta f$.

In addition, in the garden-variety multimode laser, the random phases are likely to vary slowly with time as well. This introduces yet an additional degree of randomness to the multimode laser output. To avoid such fluctuations and obtain a well-defined output, one can either utilize single-mode lasers with narrow spectra, as in Section 1.3, or mode-locked lasers with narrow pulses and broad spectra.

It is also worth noting that the carrier frequency ω_0 is left arbitrary in this very simple treatment. Indeed, in many mode-locked lasers, the carrier frequency is allowed to drift. On the other hand, for some purposes it is important to stabilize and know the carrier frequency precisely. These issues are discussed in Section 7.5.

1.5 FOURIER SERIES AND FOURIER TRANSFORMS

We shall have many occasions where we wish to describe pulses in terms of a frequency-domain representation. We encountered one example in Section 1.4, where we wrote a mode-locked periodic pulse train as a summation over the longitudinal cavity modes. In this section we briefly review Fourier series and Fourier transforms, which are the mathematical tools used to convert between time- and frequency-domain representations. For more detail, see texts such as [11,12]. The key point is that any time-dependent signal can be written as a superposition or summation of sines and cosines (or complex exponentials) with different frequencies.

1.5.1 Analytical Aspects

If a function $f(t)$ is *periodic* with period T, we can write it as a Fourier series:

$$f(t) = \sum_{n=-\infty}^{\infty} F_n e^{jn\Delta\omega t} \tag{1.77}$$

where $\Delta\omega = 2\pi/T$ is the [angular] frequency. The F_n are the Fourier amplitudes or Fourier coefficients and can be obtained from the time-domain signal $f(t)$ as follows[3]:

$$F_n = \frac{1}{T}\int_0^T f(t)e^{-jn\Delta\omega t}\,dt \tag{1.78}$$

In the case of an aperiodic time-domain function, we can consider that the period T goes to ∞. We then have the frequency spacing $\Delta\omega \to 0$, and therefore we replace the discrete variable $n\,\Delta\omega$ with a continuous variable ω. This results in the Fourier transform:

$$f(t) = \frac{1}{2\pi}\int_{-\infty}^{\infty} F(\omega)e^{j\omega t}\,d\omega \tag{1.79a}$$

and

$$F(\omega) = \int_{-\infty}^{\infty} f(t)e^{-j\omega t}\,dt \tag{1.79b}$$

$F(\omega)$ is known as the Fourier transform of $f(t)$, and $f(t)$ is obtained by performing the inverse Fourier transform of $F(\omega)$.

We now review a few useful properties of Fourier transforms, most of which we state without proof. For all of the following we assume that $f(t)$ and $F(\omega)$ are a Fourier transform pair.

- *Reality condition.* If $f(t)$ is a real function, which it will be whenever it represents an actual physical observable, $F(-\omega) = F^*(\omega)$.

[3] Instead of integrating from 0 to T, one can get the same results by integrating over any other interval of duration T (e.g., $-T/2$ to $T/2$).

- *Scaling formula:*

$$\text{If } h(t) = f(at), \quad \text{then } H(\omega) = \frac{1}{a} F\left(\frac{\omega}{a}\right) \tag{1.80}$$

- *Time-delay formula:*

$$\text{If } h(t) = f(t-\tau), \quad \text{then } H(\omega) = F(\omega) e^{-j\omega\tau} \tag{1.81}$$

- *Frequency-offset formula:*

$$\text{If } h(t) = f(t) e^{j\omega_0 t}, \quad \text{then } H(\omega) = F(\omega - \omega_0) \tag{1.82}$$

- *Convolution formula.* The convolution of two functions $f(t)$ and $g(t)$ is denoted $f(t) * g(t)$ and is defined by

$$f(t) * g(t) = \int dt'\, f(t') g(t - t')$$

The convolution formula states that

$$\text{if } h(t) = f(t) * g(t) \qquad \text{then } H(\omega) = F(\omega) G(\omega) \tag{1.83}$$

- *Parseval's theorem.* We know that the intensity $I(t)$ of a pulse whose electric field profile is $f(t)$ is proportional to $|f(t)|^2 = f(t) f^*(t)$. Recall that the units of intensity are W/m^2. The pulse energy is given by the time-integrated intensity integrated over the cross-sectional area. Parseval's theorem says that

$$\int f(t) f^*(t)\, dt = \frac{1}{2\pi} \int F(\omega) F^*(\omega)\, d\omega \tag{1.84}$$

Therefore, the time-integrated intensity is equal to the frequency-integrated intensity, except for a multiplicative factor. For this reason the quantity $|F(\omega)|^2 = F(\omega) F^*(\omega)$ is called the *power spectral density*.

The use of these formulas will be illustrated as they are needed. We do provide a few examples of the Fourier transform:

1. $f(t) = \delta(t)$, where $\delta(t)$ is the delta function or unit impulse function. Recall that $\delta(t) = 0$ for $t \neq 0$, $\delta(t) = \infty$ for $t = 0$, and $\int_{-\infty}^{\infty} dt\, \delta(t) = 1$. By substitution into eq. (1.79b), we find that $F(\omega) = 1$.
2. If $f(t) = e^{j\omega_0 t}$, then $F(\omega) = 2\pi\delta(\omega - \omega_0)$. This is verified by plugging into eq. (1.79a).

3. $f(t)$ is a Gaussian, $f(t) = e^{-t^2/t_p^2}$. Then

$$F(\omega) = \int dt\, e^{-t^2/t_p^2}\, e^{-j\omega t} = \int dt\, e^{-\left[(t+j\omega t_p^2/2)^2/t_p^2\right]}\, e^{-\omega^2 t_p^2/4}$$

Using the substitution $u = (t + j\omega t_p^2/2)/t_p$ and $\int_{-\infty}^{\infty} du\, e^{-u^2} = \sqrt{\pi}$, we obtain

$$F(\omega) = t_p\sqrt{\pi}\, e^{-\omega^2 t_p^2/4}$$

The procedure we have used above, called *completing the square*, is very useful for evaluating Fourier transforms of Gaussian functions.

Finally, we frequently write a pulse in terms of a slowly varying envelope function times an optical carrier term:

$$e(t) = \mathrm{Re}\left\{a(t)\ e^{j\omega_0 t}\right\} = \frac{1}{2}\left[a(t)\, e^{j\omega_0 t} + a^*(t)\, e^{-j\omega_0 t}\right] \tag{1.85}$$

The spectrum $E(\omega)$ is then given by

$$E(\omega) = \frac{1}{2}\left[A(\omega - \omega_0) + A^*(-\omega - \omega_0)\right] \tag{1.86a}$$

where

$$A(\omega) = \int_{-\infty}^{\infty} a(t) e^{-j\omega t}\, dt \tag{1.86b}$$

is the Fourier transform of the envelope function $a(t)$. Equation (1.86a) is sketched in Fig. 1.9. Separating the field into envelope and carrier terms is most useful when (as in Fig. 1.9) the bandwidth of $A(\omega)$ is much less than the carrier frequency ω_0. In the time domain, this means that the envelope is much longer than the optical cycle.

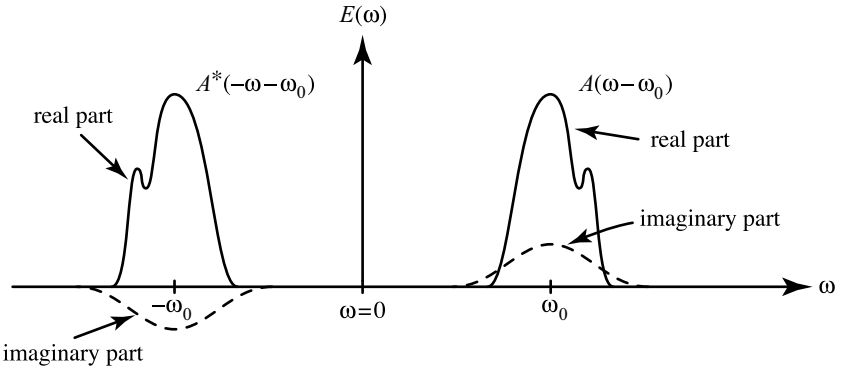

Figure 1.9 Double-sided spectrum corresponding to eq. (1.86a).

The pulse $e(t)$ can be obtained directly by performing the inverse Fourier transform of the double-sided spectrum described by eq. (1.86a) or from the single-sided spectrum using the formula

$$e(t) = \mathrm{Re}\left\{ \frac{1}{2\pi} \int A(\omega - \omega_0)\, e^{j\omega t}\, d\omega \right\} \tag{1.87}$$

1.5.2 Computational Aspects

Fourier transform methods are frequently used for computations involving ultrashort pulses. Accordingly, we introduce briefly some relevant points relating to numerical computations of Fourier transforms. For detailed discussion, see [13].

Usually computations involving a continuous-time function $f(t)$ involve only samples of $f(t)$ at a set of discrete times t_n. Let us assume that we have N evenly spaced samples with time spacing Δ, so that $t_n = n\Delta$. We designate the sample values as $f_n = f(t_n)$ for $n = 0, 1, \ldots, N-1$. The Fourier transform of $f(t)$ is then computed numerically as

$$F_k = \sum_{n=0}^{N-1} f_n e^{-2\pi jnk/N} \tag{1.88}$$

Equation (1.88) is formally called the *discrete Fourier transform*. The inverse discrete Fourier transform is given by

$$f_n = \frac{1}{N} \sum_{k=0}^{N-1} F_k e^{2\pi jnk/N} \tag{1.89}$$

Indices n and k take on integer values in the range $0, 1, \ldots, N-1$.

Discrete Fourier transform routines are widely available in numerical computing software. Practically, it is preferred to choose the vector length N to be a power of 2. This allows the numerical package to evaluate the discrete Fourier transform using the fast Fourier transform (FFT) algorithm, which dramatically reduces computing time. Although the relationship to the continuous-time Fourier transform may appear to be straightforward, several points must be kept in mind if one is to obtain sensible computational results. These points include the following:

- Although the f_n vector contains a sequence of samples of the time-domain function $f(t)$, it does not explicitly provide information on the sampling times t_n or the sampling interval. Similarly, the vector of Fourier amplitudes F_k does not explicitly stipulate the frequencies at which the spectrum is sampled. Hence, time and frequency vectors must be tracked by the user as auxiliary information. Note, however, that time and frequency vectors are related. If the sampling interval is known to be Δ, the time vector represents a total time span $N\Delta$; the frequency vector ν_k represents a total frequency span $1/\Delta$, with $\nu_k = k/N\Delta$ and spacing $1/N\Delta$ between frequency samples. Here frequency refers to $\nu = \omega/2\pi$ and is measured in hertz (as opposed to angular frequency ω measured in rad/s).

- Inspection of eqs. (1.88) and (1.89) reveals that if indices n and k were allowed to extend beyond the stipulated range, f_n and F_k would be periodic sequences with period N. f_n and F_k for n and k in the range $0, 1, \ldots, N-1$ would each then represent one period of the corresponding periodic sequences. For signals that are time-limited to duration less than $N\Delta$, or frequency-limited to bandwidth less than $1/\Delta$, meaning that the signal is nonzero only over a range of samples of length less than N, this is of little consequence. However, for signals that are not time- or frequency-limited in this way, signal content appearing at the end of the time (or frequency) vector effectively wraps around to appear at the beginning of the vector.
- Consider a continuous-time signal $f(t)$ that is frequency-limited such that its spectrum is zero for all frequencies outside the region $-B \leq \nu \leq B$. A well-known theorem states that all information about $f(t)$ is retained in its sampled representation provided that the sampling interval satisfies $\Delta \leq 1/2B$. This requirement, called the *Nyquist criterion*, is equivalent to specifying a minimum of two samples within each period of the highest-frequency component of the frequency-limited signal. Conversely, when the Nyquist criterion is not satisfied, information is lost. In the context of our discussion on the discrete Fourier transform, we note that if F_k is frequency-limited to a bandwidth less than $1/\Delta$, we have $2B < 1/\Delta$, and the Nyquist criterion is satisfied. Accordingly, in setting up an F_k vector for a computation, it is usually advisable to ensure that the nonzero values of F_k fit comfortably within the length of the vector. If necessary, this can be accomplished by zero padding the F_k vector, which is equivalent in the time domain to decreasing the sample interval (increasing the sample rate).
- For similar reasons it is usually advisable to make sure that the nonzero values of f_n fit comfortably within the vector length as well. Again this can be accomplished by zero padding if needed.
- Inspection of eqs. (1.88) and (1.89) also shows that time $t = 0$ of the physical continuous-time function $f(t)$ and frequency $\nu = 0$ of the continuous-frequency function $F(\omega)$ correspond to the first point in the f_n and F_k vectors, respectively (i.e., $t_0 = 0$ and $\nu_0 = 0$). For a signal with spectrum centered at $\nu = 0$, the "right" half of the spectrum appears at the beginning of the vector; the "left" half of the spectrum wraps around and appears at the end of the vector. A similar statement is true for a signal centered at $t = 0$ in the time domain.
- If, instead, one inadvertently positions an input spectrum so that it is centered in the frequency vector, then upon performing the inverse transform, one will notice that the expected time-domain signal is multiplied by a mysterious $(-1)^n$ function. That is, data points have alternating signs, which is equivalent to a π phase shift between points. The explanation is that the discrete Fourier transform "interprets" a shift in the positioning of the input spectrum as an actual frequency shift. Centering the input spectrum amounts to a frequency shift of $1/2\Delta$ in real units. This corresponds to a period of 2Δ in time units, equivalent to two sample intervals.
- Similarly, if one inadvertently positions an input time-domain signal so that it is centered in the time vector, then upon performing the forward transform, one will notice that the expected spectrum is multiplied by a $(-1)^k$ function. The explanation here is that a time shift in the input signal gives rise to a sampled linear phase variation in its frequency representation (F_k). For a time shift of $N\Delta/2$, the linear spectral phase amounts to a π phase shift per frequency sample.

PROBLEMS

1.1. As a review of complex notation, prove eq. (1.32).

1.2. Derive expressions for the saturated and small-signal gain of a three-level atom. Your analysis should parallel the analysis given in Section 1.3.2 for a four-level atom, but with level 4 missing. Assume that stimulated emission occurs between levels 3 and 1 and that the population in level 3 relaxes spontaneously to level 1 with time constant τ_G. Plot a family of curves for the saturated gain as a function of W (different curves represent different values of S) for both three- and four-level atoms. Comment on the main differences in gain behavior of three- and four-level atoms and on the implications for laser operation.

1.3. Analyze the gain of a two-level atom. Now there is only one laser field, denoted W. What is the gain as a function of W and τ_G, and how does this differ from three- and four-level atoms? Explain why lasers are never based on two-level atoms.

1.4. In this problem we explore the steady-state laser oscillation condition by analyzing an optical transmission resonator with gain. The setup is similar to Fig. 1.1a, but with a plane-wave field E_{in} with frequency ω incident on mirror r_1 from the left and with r_1 allowed to take on arbitrary reflectivity. The output field emerging from mirror r_2 may be written

$$E_{\text{out}} = E_{\text{in}} t_1 t_2 \sum_{n=0}^{\infty} (r_1 r_2)^n \, e^{(2n+1)g} \, e^{-(2n+1)j\omega l/c}$$

where e^g and l are the single-pass gain and optical path length, respectively, and $t_i = \sqrt{1 - r_i^2}$ is a field transmission coefficient.

(a) Assuming zero gain ($g = 0$), work out a formula for the intensity transmission coefficient $|E_{\text{out}}/E_{\text{in}}|^2$. [*Hint:* Equation (1.74) may come in handy.] Assuming a symmetric resonator ($r_1 = r_2$), plot $|E_{\text{out}}/E_{\text{in}}|^2$ as a function of ω for several values of r_1, ranging from 90 to 99%. Comment on key features in your plots, including linewidths and trends with increasing r_1.

(b) Repeat part (a) but now include gain in the resonator. Plot $|E_{\text{out}}/E_{\text{in}}|^2$ vs. ω for various values of g below the laser oscillation condition. Comment on the behavior of your plots as the gain increases toward the oscillation condition. Also explain how the phase condition shows up in your plots.

1.5. Verify by direction substitution that the Gaussian beam given by eq. (1.59) is a solution of the paraxial wave equation.

1.6. A mode-locked laser generates pulses with 10^5 W of peak power. Spatially the laser output is a Gaussian beam. If the beam is focused in air to a diameter of 10 μm (at e^{-2} points of the intensity), give the peak intensity and the corresponding peak electric field amplitude.

1.7. A mode-locked laser usually has a smooth frequency spectrum. Consider a Gaussian spectrum given by

$$A(\tilde{\omega}) = e^{-\tilde{\omega}^2/(\Delta\Omega)^2} \sum_m \delta(\tilde{\omega} - m\,\Delta\omega)\, e^{j\phi_m}$$

where $\tilde{\omega} = \omega - \omega_0$.

(a) Assuming constant spectral phase, $\phi_m = 0$, work out the expression for the time-domain complex envelope function $a(t)$. (*Hint:* The Fourier transform of a periodic train of evenly spaced, equal-amplitude delta functions is a periodic train of evenly spaced, equal-amplitude delta functions. This is shown most easily using Fourier series.)

(b) Use a computer and an FFT algorithm to evaluate the time-domain envelope function $a(t)$ for $\Delta\Omega/2\pi = 10\,\text{GHz}$, $\Delta\omega/2\pi = 100\,\text{MHz}$, and $\phi_m = 0$. Plot the spectral amplitude function $A(\tilde{\omega})$ and the temporal intensity and phase. Give the pulse duration (intensity full width at half maximum). Discuss how the setup of your array representing $A(\tilde{\omega})$ determines the number of pulses in the time-domain plot.

(c) Now obtain the phases ϕ_m from a random number generator. Plot two examples of the temporal intensity and phase and comment on all the key differences compared to the uniform phase case.